



1 **Measurement Report: Abundance and fractional solubilities of aerosol metals in urban**  
2 **Hong Kong: Insights into factors that control aerosol metal dissolution in an urban site**  
3 **in South China**

4 Junwei Yang,<sup>1</sup> Lan Ma,<sup>1</sup> Xiao He,<sup>2</sup> Wing Chi Au,<sup>1</sup> Yanhao Miao,<sup>1</sup> Wen-Xiong Wang,<sup>1,3</sup>  
5 Theodora Nah<sup>1,3\*</sup>

6 <sup>1</sup>*School of Energy and Environment, City University of Hong Kong, Hong Kong SAR, China*

7 <sup>2</sup>*College of Chemistry and Environmental Engineering, Shenzhen University, Shenzhen 518060, China*

8 <sup>3</sup>*State Key Laboratory of Marine Pollution, City University of Hong Kong, Hong Kong SAR, China*

9

10 \* *To whom correspondence should be addressed: Theodora Nah (Email: theodora.nah@cityu.edu.hk)*

11

12

**Abstract**

13 Water-soluble metals are known to produce greater adverse human health outcomes than their  
14 water-insoluble forms. Although the concentrations of water-soluble aerosol metals are usually  
15 limited by atmospheric processes that convert water-insoluble metals to water-soluble forms,  
16 factors that control the solubilities of aerosol metals in different environments remain poorly  
17 understood. In this study, we investigated the abundance and fractional solubilities of different  
18 metals in size-fractionated aerosols collected at an urban site in Hong Kong, and identified the  
19 factors that modulated metal solubilities in fine aerosols. The concentrations of total and water-  
20 soluble metals in fine and coarse aerosols were the highest during the winter and spring seasons  
21 due to the long-range transport of air masses by northerly prevailing winds from emission sources  
22 located in continental areas north of Hong Kong. The study-averaged metal fractional  
23 solubilities spanned a wide range for both fine (8.8 % to 70.3 %) and coarse (1.4 % to 54.3 %)   
24 aerosols, but higher fractional solubilities were typically observed for fine aerosols. Sulfate  
25 was found to be strongly associated with both the concentrations of water-soluble Cr, Fe, Co,  
26 Cu, Pb, and Mn and their fractional solubilities in fine aerosols, which implied that sulfate-  
27 driven acid processing likely played an important role in the dissolution of the water-insoluble  
28 forms for these six metals. Further analyses revealed that these strong associations were due to  
29 sulfate providing both the acidic environment and liquid water reaction medium needed for the  
30 acid dissolution process. Thus, the variability in the concentrations of water-soluble Cr, Fe, Co,  
31 Cu, Pb, and Mn and their fractional solubilities were driven by both the aerosol acidity levels  
32 and liquid water concentrations, which in turn were controlled by sulfate. These results  
33 highlight the roles that sulfate plays in the acid dissolution of metals in fine aerosols in Hong  
34 Kong. Our findings will likely also apply to other urban areas in South China, where sulfate is  
35 the dominant acidic and hygroscopic component in fine aerosols.

36

37



## 38 1. Introduction

39 Chronic exposures to atmospheric aerosols, especially those in the fine mode (PM<sub>2.5</sub>,  
40 aerosols with aerodynamic diameter  $\leq 2.5 \mu\text{m}$ ), have been linked to a myriad of deleterious  
41 effects on human health, including morbidity and excessive deaths through respiratory and  
42 cardiovascular diseases (Brook et al., 2010; Cohen et al., 2017). Some of the aerosol chemical  
43 species cause majority of the adverse human health outcomes even though they comprise a  
44 small fraction of the overall aerosol mass (Phalen, 2004; Lippmann, 2014). Metals are  
45 ubiquitous chemical species that contribute significantly to airborne aerosol toxicity even  
46 though they are typically present in aerosols in trace quantities (Costa and Dreher, 1997;  
47 Frampton et al., 1999; Ye et al., 2018; Zhao et al., 2021). Natural sources, especially mineral  
48 dust and sea spray, dominate the global sources of aerosol metals (Nriagu, 1989; Garrett, 2000;  
49 Deguillaume et al., 2005; Mahowald et al., 2018). However, anthropogenic sources such as  
50 industrial activities and vehicular traffic contribute substantial quantities of aerosol metals in  
51 urban environments (Garg et al., 2000; Adachi and Tainosho, 2004; Deguillaume et al., 2005;  
52 Lough et al., 2005; Birmili et al., 2006; Jiang et al., 2015; Mahowald et al., 2018).

53 Metals exist in aerosols in water-insoluble and water-soluble forms. Water-soluble  
54 metals have higher bioavailability and usually produce greater adverse human health outcomes  
55 than their water-insoluble forms (Heal et al., 2009; Fang et al., 2015; Gao et al., 2020). Some  
56 water-soluble transition metal ions (e.g., Fe(II), Fe(III), Cu(I), Cu(II)) are redox-active species  
57 and serve as catalysts in reaction cycles (e.g., Fenton-like reactions) to enhance the *in vivo*  
58 production of reactive oxygen species (ROS) (e.g., OH $\cdot$ , HO $_2\cdot$ , H $_2$ O $_2$ ), which subsequently  
59 induce the physiological oxidative stress and inflammation involved in a variety of chronic and  
60 acute diseases (Bresgen and Eckl, 2015; Lakey et al., 2016; Bates et al., 2019). A recent  
61 epidemiologic study reported that water-soluble Fe concentrations in PM<sub>2.5</sub> showed strong  
62 correlations with cardiovascular-related emergency department visits in Atlanta (Ye et al.,  
63 2018). Less abundant water-soluble aerosol metals such as Cr and Pb are also known to exhibit  
64 both carcinogenic and noncarcinogenic risks to adults and children despite their small  
65 quantities (He et al., 2021).



66 Water-soluble metals also play important roles in many atmospheric processes.  
67 Atmospheric aerosol deposition is an important source of bioavailable dissolved metals in open  
68 oceans. The dissolved metals serve as nutrients, and in some cases toxins, for various aquatic  
69 species (De Baar et al., 2005; Boyd et al., 2007; Paytan et al., 2009; Jordi et al., 2012). Some  
70 transition metal ions such as Fe(III) and Mn(II) ions can facilitate the formation and aging of  
71 organic aerosols (Chu et al., 2013; Al-Abadleh, 2015; Slikboer et al., 2015; Chu et al., 2017;  
72 Al-Abadleh, 2021). The coupled redox cycling of Cu(I)/Cu(II) and Fe(II)/Fe(III) ions in  
73 aerosols has been proposed to be an important mechanism for the uptake of gas-phase HO<sub>2</sub> in  
74 aqueous aerosols, which has important implications for the tropospheric OH radical and O<sub>3</sub>  
75 budget (Mao et al., 2013; Mao et al., 2017). Mn(II)-catalyzed oxidation of SO<sub>2</sub> on aqueous  
76 aerosol surfaces reportedly contributes more than 90 % of the sulfate production during  
77 wintertime haze events in China (Wang et al., 2021).

78 Aerosol metals are primarily emitted into the atmosphere in water-insoluble forms  
79 (Nriagu, 1989). While water-soluble aerosol metals can be emitted directly into the atmosphere  
80 (Fang et al., 2015), the concentrations of water-soluble aerosol metals are likely limited by  
81 atmospheric processes that convert the water-insoluble metal forms to water-soluble forms  
82 (Mahowald et al., 2018). Given the important roles that water-soluble aerosol metals play in  
83 adverse human health outcomes and atmospheric processes, it is necessary to understand the  
84 factors that modulate the atmospheric processing, and hence the solubility, of aerosol metals.  
85 Aerosol Fe dissolution has been the focus of most previous studies. A wide range (<1 % to  
86 98 %) of fractional solubilities (ratio of the water-soluble metal mass concentration to the total  
87 metal mass concentration) has been reported for Fe in atmospheric aerosols (Mahowald et al.,  
88 2018). Anthropogenic-influenced aerosols generally have higher Fe solubility than fresh  
89 mineral dust (Sedwick et al., 2007; Schroth et al., 2009; Oakes et al., 2012). However, Fe  
90 solubility varies substantially in aerosols in different urban environments with high levels of  
91 anthropogenic activities (e.g., 1 % to 12 % in four cities in East China (Zhu et al., 2020) vs.  
92 around 20 % to 50 % in Hong Kong, South China (Jiang et al., 2014; Jiang et al., 2015).  
93 Although there are a number of atmospheric processes that can influence aerosol metal  
94 solubilities, acid processing and the formation of stable Fe-organic complexes are two key



95 chemical processes known to enhance aerosol Fe dissolution (Deguillaume et al., 2005; Ingall  
96 et al., 2018; Tao and Murphy, 2019; Giorio et al., 2022). At present, it remains difficult to  
97 explain the variability of aerosol Fe solubility in urban environments since the extent to which  
98 aerosol Fe dissolution is controlled by factors such as aerosol acidity and/or the presence of  
99 organic ligands (e.g., oxalate) in different urban environments is still not well understood. Even  
100 less is known about the factors that control the solubilities of other aerosol metals beyond Fe.

101 Hong Kong is a highly developed, densely populated city in the Guangdong-Hong  
102 Kong-Macau Great Bay Area (GBA) urban agglomeration, which is a large business and  
103 economic hub located in the southern part of China. While there have been some studies on the  
104 fractional solubilities of various aerosol metals in Hong Kong (Jiang et al., 2014; Jiang et al.,  
105 2015), to the best of our knowledge, there has not been a study that has investigated the factors  
106 that control the solubilities of aerosol metals in Hong Kong. In this study, we investigated the  
107 abundance and fractional solubilities of ten metals (Fe, Cu, Al, V, Cr, Mn, Co, Ni, Cd, and Pb)  
108 in aerosols at an urban site in Hong Kong. Our main goal is to identify the key factors that  
109 control the solubilities of metals in fine aerosols since they are believed to exert higher toxicity  
110 than coarse aerosols due to their small sizes. We focus primarily on aerosol metal dissolution  
111 through the acid processing and/or metal-organic complexation mechanisms. Hence, other  
112 aerosol species were also measured for comparisons to total and water-soluble metals. The  
113 measured aerosol inorganic ion composition was used as inputs for a thermodynamic model to  
114 determine the aerosol acidity levels, liquid water concentrations, and pH.

## 115 **2. Methods**

### 116 **2.1. Ambient sampling**

117 The sampling campaign took place at ground level next to a road in Kowloon Tong  
118 (22.3367° N, 114.1724° E). Kowloon Tong is located in the southern side of Hong Kong, and  
119 it is primarily a residential and commercial district which is close to Mongkok, one of the  
120 busiest commercial and most densely populated areas in Hong Kong with high density traffic  
121 flow. Weekly size-fractionated aerosol samples were collected on 7 March 2021 to 4 April 2021  
122 (spring season), 23 to 30 June 2021 and 7 to 14 July 2021 (summer season), 13 September



123 2021 to 11 October 2021 (fall season), and 15 December 2021 to 26 January 2022 (winter  
124 season). Back-trajectories calculations calculated by the Hybrid Split-Particle Lagrangian  
125 Integrated Trajectory (HYSPLIT) model using meteorological data from NCEP/NCAR  
126 Reanalysis (2.5° latitude-longitude grid) showed that the sampling site was under the influence  
127 of continental and marine air masses during the sampling periods, though the contributions of  
128 these air masses varied with the season (Figure S1).

129 An eleven stage Micro-Orifice Uniform Deposit Impactor (MOUDI) (Model 110, MSP  
130 Corp., USA) was used to collect and divide aerosols into different aerosol size bins under  
131 ambient conditions. Aerosols were collected on prebaked 47 mm diameter quartz filters  
132 (Tissuquartz 2500QAT-UP, Pall Corp., USA). The nominal cut points for the MOUDI eleven  
133 impactor stages were 0.056  $\mu\text{m}$ , 0.1  $\mu\text{m}$ , 0.18  $\mu\text{m}$ , 0.32  $\mu\text{m}$ , 0.56  $\mu\text{m}$ , 1.0  $\mu\text{m}$ , 1.8  $\mu\text{m}$ , 3.2  $\mu\text{m}$ ,  
134 5.6  $\mu\text{m}$ , 10  $\mu\text{m}$ , and 18  $\mu\text{m}$ . In the discussion below, for simplicity, we refer to aerosols  
135 collected on impactor stages with nominal cut points 0.056  $\mu\text{m}$ , 0.1  $\mu\text{m}$ , 0.18  $\mu\text{m}$ , 0.32  $\mu\text{m}$ ,  
136 0.56  $\mu\text{m}$ , 1.0  $\mu\text{m}$ , and 1.8  $\mu\text{m}$  as “fine aerosols”, while aerosols collected on impactor stages  
137 with nominal cut points 3.2  $\mu\text{m}$ , 5.6  $\mu\text{m}$ , 10  $\mu\text{m}$ , and 18  $\mu\text{m}$  were referred to as “coarse  
138 aerosols”. Aerosols were collected continuously for seven days (i.e., 24 hours  $\times$  7 days). This  
139 resulted in a total of four, two, four, and six weekly sets of aerosol filter samples collected  
140 during the spring, summer, fall, and winter seasons, respectively. After collection, the aerosol  
141 filter samples were immediately extracted for chemical analysis.

142 Thermodynamic model calculations used to determine the aerosol acidity levels, liquid  
143 water concentrations, and pH (Section 2.3) require gas-phase  $\text{NH}_3$  concentrations, ambient  
144 temperature and relative humidity (RH) as model inputs. Hence, weekly  $\text{NH}_3$  measurements  
145 were performed during each sampling period using four passive sampling devices (PSDs) and  
146 pre-coated collection pads (PS-100 and PS-154, Ogawa & Co., Pompano Beach, FL), except  
147 from 7 to 28 March 2021. The exposed PSD collection pads were extracted in purified  
148 deionized water (18.2  $\text{M}\Omega\text{-cm}$ ) using the protocol recommended by the manufacturer. These  
149 aqueous extracts were subsequently analyzed by ion chromatography (Section 2.2) to  
150 determine the average  $\text{NH}_3$  concentration during the sampling period. A Vantage Vue Weather  
151 Station (Model 6250, Davis Instruments, USA) was used to measure ambient temperature and



152 RH during each sampling period.

## 153 2.2. Chemical analysis

154 Each aerosol filter sample was cut into four equal pieces for chemical analysis of  
155 different chemical components. One of the four pieces was extracted in purified deionized  
156 water. The resulting aqueous extract was analyzed by a Total Organic Carbon (TOC) analyzer  
157 (TOC-VCSH, Shimadzu, Japan) to determine the concentration of water-soluble organic  
158 carbon (WSOC). The TOC analyzer has a limit of detection (LOD) of  $0.5 \text{ mg L}^{-1}$ . The second  
159 filter piece was similarly extracted in purified deionized water, and then analyzed by an ion  
160 chromatography (IC) system (Dionex ICS-1100, ThermoFisher Scientific, USA) using an  
161 isocratic method to determine the concentrations of water-soluble anions ( $\text{NO}_3^-$ ,  $\text{SO}_4^{2-}$ ,  $\text{Cl}^-$ ,  
162 and  $\text{C}_2\text{O}_4^{2-}$ ) and cations ( $\text{NH}_4^+$ ,  $\text{Na}^+$ ,  $\text{K}^+$ ,  $\text{Ca}^{2+}$ , and  $\text{Mg}^{2+}$ ). Anion separation was achieved using  
163 a  $4 \times 250 \text{ mm}$  anion exchange column (Dionex IonPac AS18, ThermoFisher Scientific, USA)  
164 equipped with a  $4 \times 50 \text{ mm}$  guard column (Dionex IonPac AG18, ThermoFisher Scientific,  
165 USA). Cation separation was achieved using a  $4 \times 250 \text{ mm}$  cation exchange column (Dionex  
166 IonPac CS12A, ThermoFisher Scientific, USA) equipped with a  $4 \times 50 \text{ mm}$  guard column  
167 (Dionex IonPac CG12A, ThermoFisher Scientific, USA).  $16 \text{ mM}$  potassium hydroxide and  $31$   
168  $\text{mM}$  methanesulfonic acid were used as eluents at a flowrate of  $1.0 \text{ mL min}^{-1}$  for the anion and  
169 cation separations, respectively. The cation IC method was also used to analyze the aqueous  
170 extracts from the exposed PSD collection pads to determine the average  $\text{NH}_3$  concentration  
171 during each sampling week. The LODs for the cation IC method were  $0.025 \text{ mg L}^{-1}$  for  $\text{NH}_4^+$ ,  
172  $\text{Na}^+$ , and  $\text{Mg}^{2+}$ , and  $0.025 \text{ mg L}^{-1}$  for  $\text{K}^+$  and  $\text{Ca}^{2+}$ . The LODs for the anion IC method were  
173  $0.125 \text{ mg L}^{-1}$  for  $\text{NO}_3^-$ ,  $\text{SO}_4^{2-}$ , and  $\text{C}_2\text{O}_4^{2-}$ , and  $0.025 \text{ mg L}^{-1}$  for  $\text{Cl}^-$ .

174 The remaining two filter pieces were used for metal analysis. One filter piece was  
175 extracted with purified deionized water in metal-free centrifuge tubes via sonication (1 hour),  
176 followed by high speed vortexing (15 minutes). The resulting aqueous extract was then  
177 acidified with  $2 \%$   $\text{HNO}_3$  prior to storage at  $4 \text{ }^\circ\text{C}$  before chemical analysis of water-soluble  
178 metals. The last filter piece was extracted via acid digestion for chemical analysis of total  
179 metals. The acid digestion protocol we employed was adapted from published protocols (Jiang



180 et al., 2014; Jiang et al., 2015). The filter piece was extracted in an acid digestion matrix (16 N  
181 HNO<sub>3</sub> and 12 N HCl at a 3:1 volume ratio) placed in a glass microwave vial using a microwave  
182 synthesizer (Initiator+, Biotage, Sweden). The microwave synthesizer's digestion temperature  
183 was ramped up to 150 °C, and then held for 15 min. This was followed by cooling and  
184 ventilation for 30 minutes. An evaporation and recovery treatment was next performed to  
185 remove Cl<sup>-</sup> from the matrix to reduce its interference during chemical analysis. The digestion  
186 solution was heated to 200 °C on a hotplate. Once the solution was observed to be almost dry,  
187 16 N HNO<sub>3</sub> was added to the solution. When the solution was observed to be almost dry the  
188 second time, 2 % HNO<sub>3</sub> was added to the solution. The resulting solution was stored at 4 °C  
189 before chemical analysis of total metals. A standard reference material of San Joaquin soil  
190 (SRM 2709a, NIST) was digested and analyzed using the same protocols to evaluate the metal  
191 recoveries. Recoveries of 59.4 % for Cr, 67.0 % for Al, 93.7 % for Fe, 93.6 % for Ni, 100.2 %  
192 for Co, 98.6 % for Pb, 95.8 % for Cu, 99.6 % for Mn, 70.5 % for V, and 94.3 % for Cd were  
193 observed.

194 The concentrations of ten water-soluble and total metals (<sup>27</sup>Al, <sup>51</sup>V, <sup>52</sup>Cr, <sup>55</sup>Mn, <sup>57</sup>Fe,  
195 <sup>59</sup>Co, <sup>60</sup>Ni, <sup>65</sup>Cu, <sup>111</sup>Cd, and <sup>208</sup>Pb) were determined by an Inductively Coupled Plasma–Mass  
196 Spectrometry (ICP–MS) instrument (NexION 1000, PerkinElmer Inc., USA). The following  
197 parameters were used for the ICP-MS instrument: 0.98 L min<sup>-1</sup> nebulizer gas flow, 1.2 L min<sup>-1</sup>  
198 auxiliary gas flow, 15 L min<sup>-1</sup> plasma gas flow, 5 mL min<sup>-1</sup> He gas flow, 1600 W RF power,  
199 35 rpm nebulizer pump rate, and 35 rpm sample pump rate. A multi-elemental calibration  
200 standard (IV-STOCK-13, Inorganic Ventures, USA) was used to quantify the ten water-soluble  
201 and total metals. An internal standard solution of <sup>115</sup>In (10 µg L<sup>-1</sup>) was added to all samples  
202 and standards to monitor analytical drift. The LODs for <sup>27</sup>Al, <sup>51</sup>V, <sup>52</sup>Cr, <sup>55</sup>Mn, <sup>57</sup>Fe, <sup>59</sup>Co, <sup>60</sup>Ni,  
203 <sup>65</sup>Cu, <sup>111</sup>Cd, and <sup>208</sup>Pb were 87 ng L<sup>-1</sup>, 0.8 ng L<sup>-1</sup>, 2.8 ng L<sup>-1</sup>, 1.6 ng L<sup>-1</sup>, 277 ng L<sup>-1</sup>, 0.7 ng L<sup>-1</sup>,  
204 4.6 ng L<sup>-1</sup>, 6.7 ng L<sup>-1</sup>, 1 ng L<sup>-1</sup>, and 0.4 ng L<sup>-1</sup>, respectively. To identify the major sources of the  
205 aerosol metals, source apportionment was performed with positive matrix factorization (PMF)  
206 (Paatero and Tapper, 1994; Paatero, 1997) using the aerosol chemical components measured  
207 by the ICP-MS and IC. Details of the PMF method used can be found in Section S1 (SI).

### 208 2.3. Thermodynamic modeling



209 The thermodynamic model ISORROPIA-II was used to determine aerosol acidity levels,  
210 liquid water concentrations, and pH (Fountoukis and Nenes, 2007). Similar to the methodology  
211 employed by Fang et al. (2017), we ran ISORROPIA-II for each of the MOUDI impactor stages  
212 that collected fine aerosols. The measured water-soluble  $\text{NH}_4^+$ ,  $\text{SO}_4^{2-}$ ,  $\text{NO}_3^-$ ,  $\text{Cl}^-$ ,  $\text{Na}^+$ ,  $\text{Ca}^{2+}$ ,  $\text{K}^+$ ,  
213 and  $\text{Mg}^{2+}$  ions for the aerosols collected on the MOUDI impactor stage, gas-phase  $\text{NH}_3$ ,  
214 ambient temperature and RH were used as model inputs. Since gas-phase  $\text{NH}_3$  measurements  
215 were not available from 7 to 28 March 2021, we used  $\text{NH}_3$  measurements from 28 March to 4  
216 April 2021 as model inputs for the spring calculations. The measured  $\text{NH}_3$  concentrations  
217 during the study ranged from  $3.60 \mu\text{g m}^{-3}$  to  $8.18 \mu\text{g m}^{-3}$ , with a study-averaged concentration  
218 of  $5.01 \pm 1.25 \mu\text{g m}^{-3}$ . ISORROPIA-II was run in “forward” mode and under the assumption  
219 that the aerosols existed in a “metastable” equilibrium state (i.e., the aerosols only existed in  
220 liquid form). These calculations assumed that the aerosols were in thermodynamic equilibrium  
221 with the gas phase. While fine aerosols satisfy this equilibrium condition, equilibrium between  
222 the gas and aerosol phases of coarse aerosols cannot be achieved due to kinetic limitations  
223 (Fountoukis et al., 2009). Thus, aerosol pH values were not calculated for coarse aerosols.

224 Fine aerosol pH values were calculated based on the molal definition (Pye et al., 2020):

$$225 \quad \text{pH} = -\log_{10} H_{aq}^+ = -\log_{10} \frac{1000H_{air}^+}{W_i+W_o} \cong -\log_{10} \frac{1000H_{air}^+}{W_i} \quad (1)$$

226 where  $H_{air}^+$  is the hydronium ion concentration per volume of air ( $\mu\text{g m}^{-3}$ ), and  $W_i$  and  $W_o$  are  
227 the aerosol liquid water concentrations ( $\mu\text{g m}^{-3}$ ) associated with inorganic and organic species,  
228 respectively.  $H_{air}^+$  and  $W_i$  are the outputs provided by ISORROPIA-II.  $W_o$  can be estimated  
229 from the WSOC measurements using the approach described in Section S2 (SI). WSOC  
230 concentrations in the size-fractionated aerosols ranged from 0 to  $4.6 \mu\text{g m}^{-3}$ . The inclusion of  
231  $W_o$  into calculations did not impact aerosol pH significantly (Figure S2). Thus, only aerosol  
232 pH values calculated using  $W_i$  will be reported here. Similar to Fang et al. (2017), lower pH  
233 values were typically calculated for aerosols collected on MOUDI impactor stages with smaller  
234 nominal cut points (i.e., these aerosols had smaller aerodynamic aerosol diameters) due to the  
235 higher mass concentrations of sulfate in these smaller aerosols. The fine aerosols were mostly  
236 acidic, with about 74 % of the calculated pH values lying between 2 and 4.



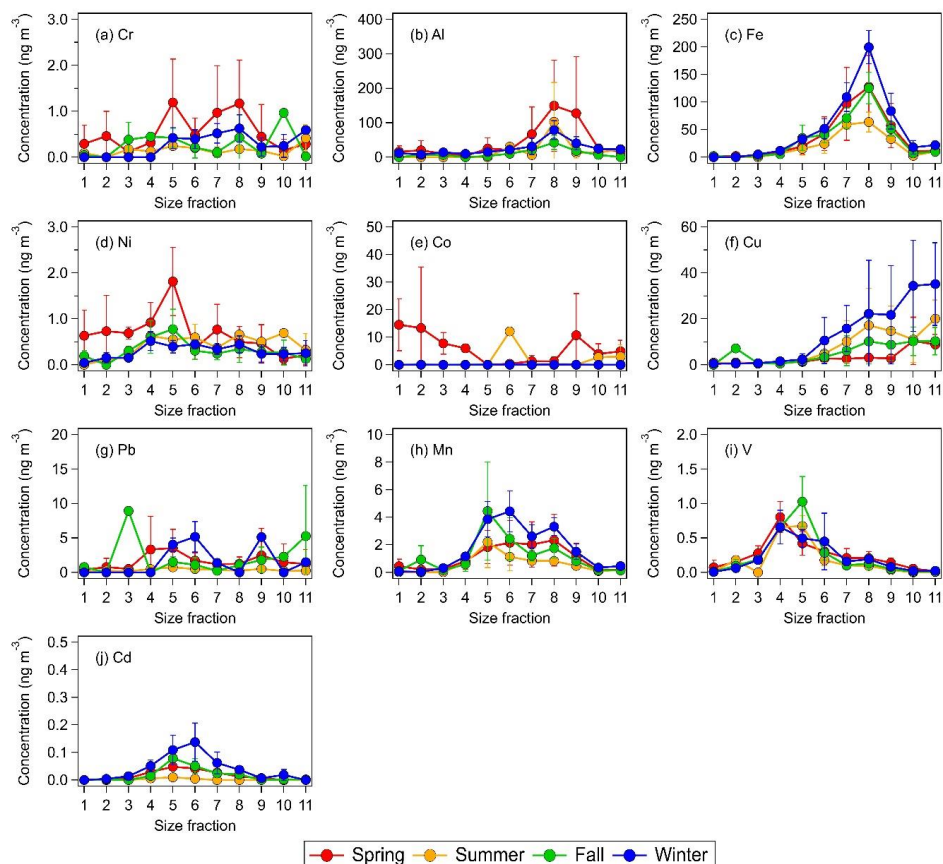


### 237 3. Results and discussion

#### 238 3.1. Total metals

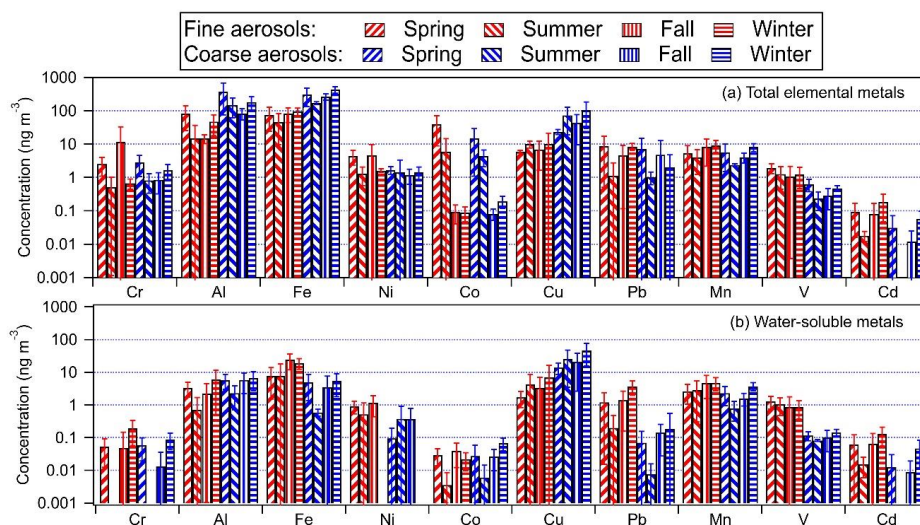
239 Figure 1 shows the seasonal average mass concentrations of the ten measured total  
240 metals in size-fractionated aerosols. The size distributions of five of the metals (Al, Fe, Mn, V,  
241 and Cd) consistently exhibited a single mode. The modes for Mn, V, and Cd were  
242 predominantly found in the fine mode, while the modes for Fe and Al were predominantly  
243 found in the coarse aerosol mode. Figure 2a shows the seasonal average concentrations of the  
244 ten measured total metals in fine and coarse aerosols. For most of the metals, higher mass  
245 concentrations were measured during the winter and/or spring seasons. This could be attributed  
246 to the long-range transport of polluted air masses by northerly prevailing winds from emission  
247 sources located in continental areas north of Hong Kong (Figure S1). The metals could be  
248 arranged in the following order based on their abundances: Fe > Al > Cu > Mn > Pb > Ni >  
249 Cr > V > Co > Cd. This order of abundance was the same for both fine and coarse aerosols.

250 The mass concentrations of the two most abundant metals, Fe and Al, were usually  
251 higher than  $10 \text{ ng m}^{-3}$  in both fine and coarse aerosols. Fe, Al, and Cu had substantially higher  
252 mass concentrations in coarse aerosols than in fine aerosols. These three metals are known to  
253 originate mainly from dust sources (e.g., mineral dust and road dust) (Hopke et al., 1980; Garg  
254 et al., 2000; Adachi and Tainosho, 2004; Lough et al., 2005; Chow et al., 2022). In contrast,  
255 Mn, Ni, V, and Cd had higher mass concentrations in fine aerosols than in coarse aerosols.  
256 These four metals are known to be consistently found in aerosols from anthropogenic sources  
257 such as vehicle and ship emissions, combustion and industrial processes (Chow et al., 2022).  
258 Pb, Cr, and Co had mostly similar concentrations in the fine and coarse aerosols.



259

260 **Figure 1:** Seasonal average concentrations of total elemental metals in size-fractionated  
261 aerosols sampled by the MOUDI with the following nominal cut points: 0.056  $\mu\text{m}$  (size fraction  
262 1), 0.1  $\mu\text{m}$  (size fraction 2), 0.18  $\mu\text{m}$  (size fraction 3), 0.32  $\mu\text{m}$  (size fraction 4), 0.56  $\mu\text{m}$  (size  
263 fraction 5), 1.0  $\mu\text{m}$  (size fraction 6), 1.8  $\mu\text{m}$  (size fraction 7), 3.2  $\mu\text{m}$  (size fraction 8), 5.6  $\mu\text{m}$   
264 (size fraction 9), 10  $\mu\text{m}$  (size fraction 10), and 18  $\mu\text{m}$  (size fraction 11). The error bars represent  
265 one standard deviation of the seasonal average value.



266

267 **Figure 2:** Seasonal average mass concentrations of (a) total metals and (b) water-soluble metals  
268 in fine (red) and coarse (yellow) aerosols. The error bars represent one standard deviation. The  
269 y axes are on logarithm scales.

270 Jiang et al. (2015) previously measured the mass concentrations of various total metals  
271 in PM<sub>2.5</sub> and PM<sub>2.5-10</sub> in Kowloon Tong. The authors carried out their measurements from 12  
272 November 2012 to 10 December 2012 (winter) and from 8 April 2013 to 13 May 2013  
273 (spring/summer). To gain some insights into how the aerosol metal concentrations at this urban  
274 site have changed since 2012/2013, we compared the average mass concentrations of total  
275 metals in fine and coarse aerosols measured in this study to those measured by Jiang et al.  
276 (2015). As shown in Table S1, lower mass concentrations were measured in fine (30 % to 94 %  
277 lower) and coarse (7 % to 80 % lower) aerosols for most of the metals in this study. While the  
278 lower aerosol metal mass concentrations could be partly attributed to lower levels of  
279 anthropogenic activities in 2021/2022 due to COVID-19, it is likely that the implementation of  
280 numerous local and regional air pollution policies to reduce industrial and transport-related  
281 emissions over the last decade contributed largely to this decrease. For instance, industrial  
282 upgrades resulting from the implementation of the “double transfer” policy (industry and labor  
283 transfer away from primary industries) in Guangdong likely caused the decline in the mass  
284 concentrations of metals that are typically associated with industrial activities such as Cu and



285 Mn (Zhong et al., 2013; Chow et al., 2022). In addition, government policies driving the switch  
286 to cleaner fuels for energy generation and transport in Hong Kong and the GBA likely caused  
287 the decline in the mass concentrations of metals such as Pb, Ni, V, and Fe. Interestingly, higher  
288 mass concentrations were measured for Fe and Cu in coarse aerosols in this study compared to  
289 those measured by Jiang et al. (2015). Fe and Cu in coarse aerosols have previously been linked  
290 to resuspended road dust from brake and tire wear (Garg et al., 2000; Adachi and Tainosho,  
291 2004; Lough et al., 2005). Based on publicly available government data ([www.td.gov.hk](http://www.td.gov.hk)), the  
292 number of registered motor vehicles in Hong Kong has increased by about 34 % over the last  
293 decade. It is possible that the higher Fe and Cu mass concentrations in coarse aerosols in this  
294 study were due to increased contributions from road dust as a result of increased vehicle fleet  
295 size at the urban site.

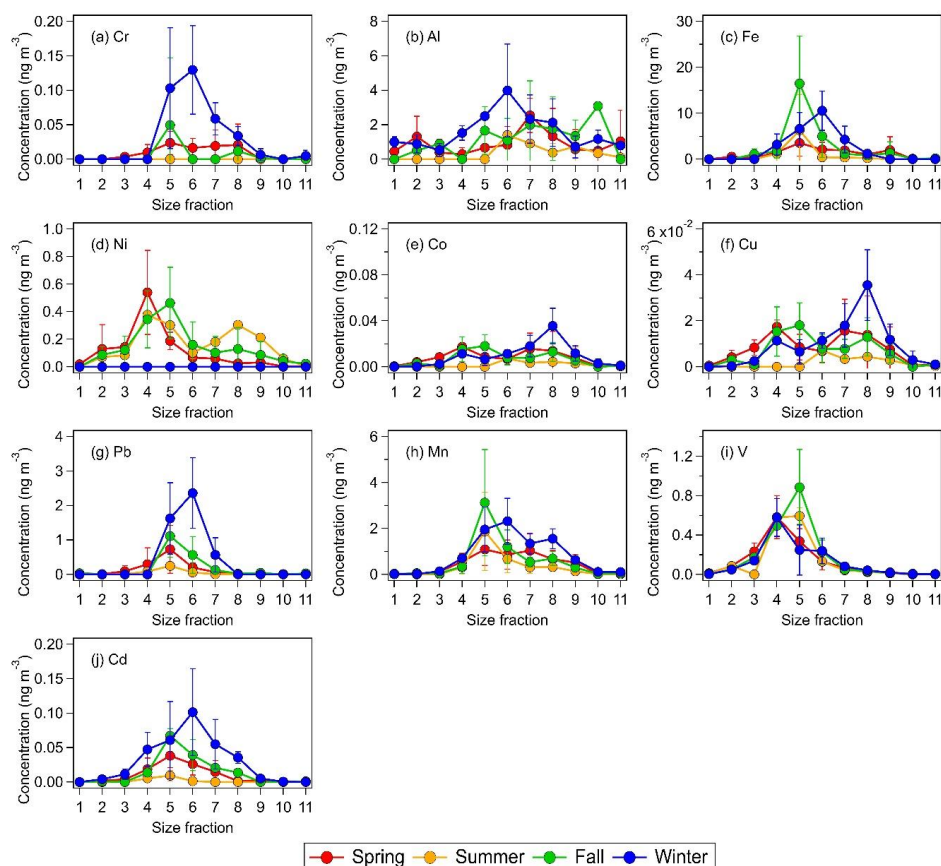
296 A PMF source apportionment analysis was performed to determine the major sources  
297 of aerosol metals measured in this study (Section S1). A five-factor solution was selected since  
298 it gave the most reasonable factor profiles and had high stability. The five factors were  
299 identified as “sea salt”, “dust”, “ship emissions”, “industrial factor 1”, and “industrial factor 2”  
300 based on the tracer species with the highest mass loadings in each factor (Figure S3). Figure  
301 S4 shows the seasonal mass contributions of each source to each metal species in coarse and  
302 fine aerosols. Metals with large fractions in the dust and sea salt source factor profiles generally  
303 had higher mass concentrations in coarse aerosols. Conversely, metals with large fractions in  
304 the ship emissions and industrial source factor profiles generally had higher mass  
305 concentrations in fine aerosols. Higher mass contributions were usually observed in the winter  
306 and/or spring seasons, which could be attributed to the long-range transport of polluted air  
307 masses by northly prevailing winds from emission sources located in continental areas north  
308 of Hong Kong (Figure S1).

### 309 **3.2. Water-soluble metals**

310 Figure 3 shows the seasonal average mass concentrations of water-soluble metals in  
311 size-fractionated aerosols. The size distribution of six of the water-soluble metals (Cr, Fe, Pb,  
312 Mn, V, and Cd) mostly exhibited a single mode, all of which were found in the fine aerosol



313 mode. Fe, Mn, V, and Cd exhibited a single mode for both their total and water-soluble  
314 components (Figures 1 and 3). Of these four metals, only the modes of total and water-soluble  
315 Fe showed obvious differences, with total Fe exhibiting a mode at around  $3.2\ \mu\text{m}$  (size fraction  
316 8) and water-soluble Fe exhibiting a mode at around  $0.56\ \mu\text{m}$  to  $1.0\ \mu\text{m}$  (size fractions 5 to 6).  
317 The modes of total and water-soluble Cu also showed obvious differences. While the mode of  
318 total Cu was at  $\geq 18\ \mu\text{m}$  (Figure 1f), the modes of water-soluble Cu were found at substantially  
319 smaller aerosol sizes (Figure 3f).



320

321 **Figure 3:** Seasonal average concentrations of water-soluble metals in size-fractionated aerosols  
322 sampled by the MOUDI with the following nominal cut points:  $0.056\ \mu\text{m}$  (size fraction 1),  $0.1$   
323  $\mu\text{m}$  (size fraction 2),  $0.18\ \mu\text{m}$  (size fraction 3),  $0.32\ \mu\text{m}$  (size fraction 4),  $0.56\ \mu\text{m}$  (size fraction  
324 5),  $1.0\ \mu\text{m}$  (size fraction 6),  $1.8\ \mu\text{m}$  (size fraction 7),  $3.2\ \mu\text{m}$  (size fraction 8),  $5.6\ \mu\text{m}$  (size



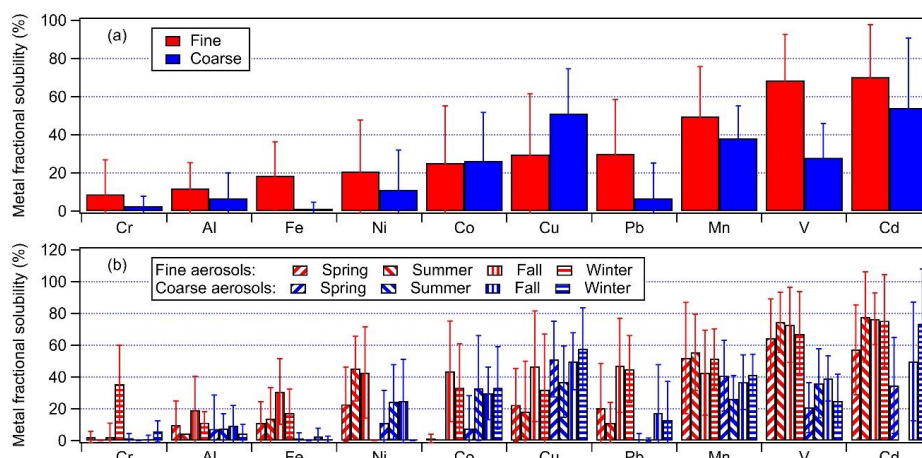
325 fraction 9), 10  $\mu\text{m}$  (size fraction 10), and 18  $\mu\text{m}$  (size fraction 11). The error bars represent one  
326 standard deviation of the seasonal average value.

327 Figure 2b shows the seasonal average mass concentrations of water-soluble metals in  
328 fine and coarse aerosols. Similar to the total metals, higher mass concentrations of water-  
329 soluble metals were usually measured during the winter and/or spring seasons. With the  
330 exception of Cu, the water-soluble metals usually had higher mass concentrations in fine  
331 aerosols than in coarse aerosols. The water-soluble metals generally had the same order of  
332 abundance as the total metals with some slight variations. The mass concentrations of water-  
333 soluble metals generally correlated with the mass concentrations of total metals (Table S2).  
334 This indicated that the water-soluble metals were largely derived from their total metals  
335 through atmospheric processing, and/or that water-soluble and water-insoluble metals have the  
336 same emission sources. For most of the metals, correlations between the mass concentrations  
337 of water-soluble and total metals were higher for fine aerosols than for coarse aerosols. This  
338 could be due to enhanced metal dissolution in fine aerosols via acid processing and/or the  
339 formation of stable metal-organic complexes, which are two atmospheric chemical processes  
340 that play key roles in influencing the solubilities of aerosol metals in many locations. This is  
341 because acidic inorganic species that promote acid processing and organic species that can  
342 serve as organic ligands are typically present in larger quantities in fine aerosols than in coarse  
343 aerosols. It is also possible that differences in metal mineralogy and atmospheric processing  
344 mechanisms in fine vs. coarse aerosols could have contributed to differences in the metal  
345 dissolution rates (Oakes et al., 2012; Longo et al., 2016; Ingall et al., 2018).

346 Figure 4 shows the study-averaged fractional solubilities for the ten metals in fine and  
347 coarse aerosols. The study-averaged metal fractional solubilities spanned a wide range for both  
348 fine (8.8 % to 70.3 %) and coarse (1.4 % to 54.3 %) aerosols. With the exception of Cu and Co,  
349 the metals generally exhibited higher fractional solubilities in fine aerosols compared to coarse  
350 aerosols. The aerosol size-dependent metal fractional solubility could be explained by  
351 differences in the aerosol composition and metal mineralogy, which resulted in different metal  
352 dissolution rates and/or mechanisms for aerosols of different sizes. Our observations of mostly  
353 higher metal fractional solubilities in fine aerosols are consistent with previous studies



354 conducted in Hong Kong (Jiang et al., 2014; Jiang et al., 2015). No season-dependent trend  
355 was observed for the metal fractional solubilities.



356  
357 **Figure 4:** (a) Study-averaged fractional solubilities of metals in fine and coarse aerosols. (b)  
358 Seasonal average fractional solubilities of metals in fine and coarse aerosols. The error bars  
359 represent one standard deviation.

360 Some studies have reported that aerosol metal fractional solubilities will exhibit inverse  
361 relationships with the total metal concentrations as a result of atmospheric processing (Baker  
362 and Jickells, 2006; Sholkovitz et al., 2012; Mahowald et al., 2018; Shelley et al., 2018; Zhang  
363 et al., 2022). There was significant scatter in many of our datasets (Figure S5), which made it  
364 difficult to discern some of the relationships between the metal fractional solubilities and total  
365 metal concentrations. Inverse relationships between the fractional solubility and total metal  
366 concentration were noticeable for Cr, Al, Fe, Ni, Cu, Pb, and Mn. However, inverse  
367 relationships between the Co, V, and Cd fractional solubilities and their total metal  
368 concentrations were less noticeable due to their low concentrations and scatter in their datasets.  
369 A number of factors could have contributed to the scatter in the datasets. For instance, the  
370 scatter could be a result of the total and water-soluble metal concentrations being substantially  
371 different in individual aerosol particles, which would not be captured by the bulk chemical  
372 analysis performed in this study (Oakes et al., 2012; Longo et al., 2016; Ingall et al., 2018).  
373 The metal dissolution rates in individual aerosol particles could also be significantly different



374 due to differences in metal mineralogy, aerosol acidity levels, presence of organic ligands etc.  
375 in individual aerosol particles.

### 376 **3.3. Factors that control the aerosol metal solubilities**

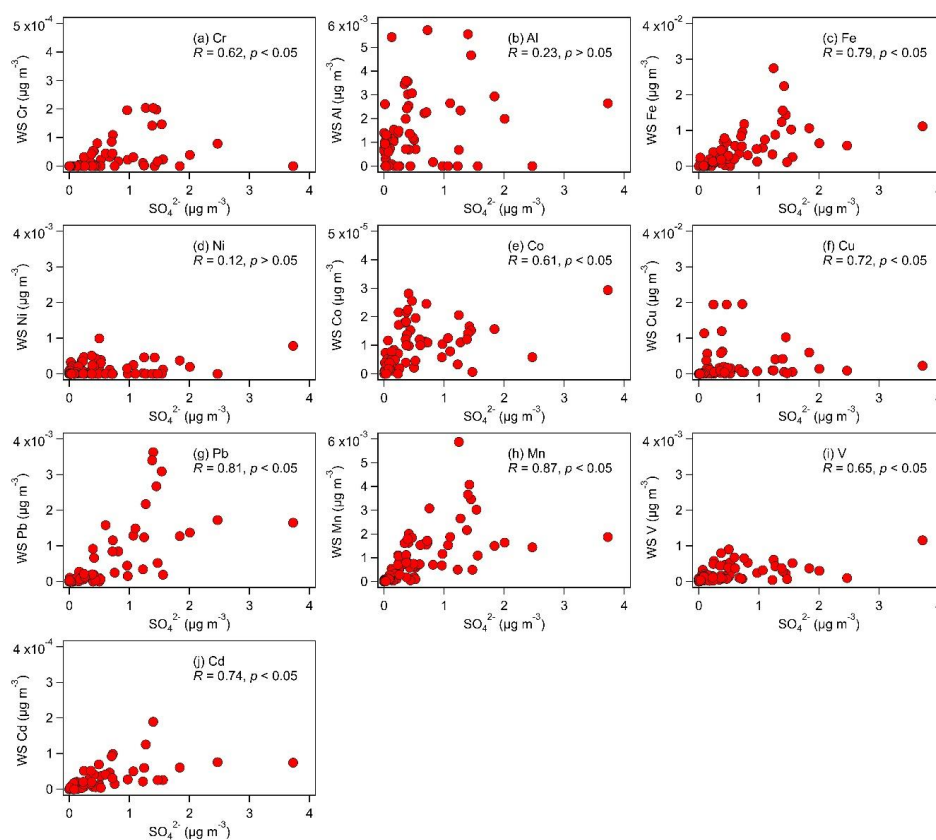
377 Here, we identify the factors that control metal solubilities in fine aerosols since they  
378 are believed to exert higher toxicity than coarse aerosols due to their small sizes. Our analyses  
379 focus on aerosol metal dissolution via metal-organic complexation reactions and acid  
380 processing, which are two atmospheric chemical processes believed to drive aerosol metal  
381 dissolution in most environments. Laboratory studies have shown that the presence of organic  
382 ligands enhances Fe dissolution in aerosols (Paris et al., 2011; Chen and Grassian, 2013; Paris  
383 and Desboeufs, 2013; Wang et al., 2017). Water-soluble dicarboxylic acids, especially oxalate,  
384 form stable complexes with Fe ions, which will lower the energy barrier for Fe dissolution.  
385 While evidence of organic ligand-promoted metal dissolution in ambient aerosols has been less  
386 conclusive, recent field studies compared the oxalate and water-soluble Fe concentrations to  
387 show that the presence of organic ligands could contribute to aerosol Fe solubility. For instance,  
388 strong positive correlations between oxalate and water-soluble Fe mass concentrations were  
389 observed for PM<sub>2.5</sub> collected at six urban and rural sites in Canada (Tao and Murphy, 2019).  
390 The Fe fractional solubility was also observed to be positively correlated with the molar ratio  
391 of oxalate and Fe for PM<sub>2.5</sub> collected at a suburban site in Qingdao, China (Zhang et al., 2022).

392 To investigate whether organic ligands influenced aerosol metal solubilities in this study,  
393 we attempted to measure oxalate in the size-fractionated aerosol samples using IC. However,  
394 we could not detect oxalate, which indicated that the concentrations of oxalate (if present) were  
395 below the detection limits of our IC instrument. Even though oxalate was not detected in our  
396 size-fractionated aerosol samples, the possibility that organic ligand-promoted dissolution  
397 contributed partly to the aerosol metal solubilities cannot be discounted completely. Oxalate  
398 concentrations of up to about 0.5  $\mu\text{g m}^{-3}$  have previously been reported in PM<sub>2.5</sub> in Hong Kong.  
399 In addition, a recent study reported the copresence of Fe and oxalate in individual aerosol  
400 particles at a suburban site in Hong Kong using single particle mass spectrometry (Zhou et al.,  
401 2020). However, organic ligand-promoted metal dissolution is a slow process, and it plays a





402 minor role in metal dissolution under low pH conditions (Zhu et al., 1993). The fine aerosols  
403 collected in this study were mostly acidic, with about 60 % of the calculated pH values being  
404 less than 3. This suggested that organic ligand-promoted dissolution may have played a minor  
405 role in enhancing aerosol metal solubilities in this study due to the acidic nature of the aerosols.



406

407 **Figure 5:** Relationships between the mass concentrations of water-soluble (WS) metals and  
408 sulfate in fine aerosols. Only data with non-zero total metal concentrations were used in the  
409 figures. Also shown are the spearman correlation coefficients for each relationship.

410 The acidic nature of the aerosols raises the possibility that acid processing played a  
411 major role in enhancing aerosol metal solubilities. During acid processing, acidic species have  
412 to overcome the buffering capacity of the aqueous aerosol particle to raise the aerosol acidity  
413 level to the point where the dissolution of metal species is thermodynamically favored. Since



414 sulfate is the main aqueous-phase acidic species in fine aerosols in Hong Kong, we first  
415 analyzed the relationships between the concentrations of water-soluble metals and sulfate.  
416 Figure 5 shows that despite the scatter in the datasets, the concentrations of water-soluble  
417 metals were positively correlated with the concentration of sulfate, though the correlations  
418 between the concentrations of sulfate and water-soluble Al and Ni were not statistically  
419 significant. These positive correlations could be due, in part, to the water-soluble metals and  
420 sulfate precursor (i.e., SO<sub>2</sub>) being emitted from the same sources. However, the masses of  
421 primary water-soluble aerosol metals are not known. The positive correlations could also be  
422 due to the role that sulfate plays in aerosol metal dissolution during acid processing.

423 To investigate the role that sulfate played in controlling aerosol metal solubilities, we  
424 analyzed the relationships between the metal fractional solubilities and sulfate concentration.  
425 Analyses of the correlations between the metal fractional solubilities and sulfate concentration  
426 (Table 1 and Figure 6) indicated that the Cr, Fe, Co, Cu, Pb, and Mn fractional solubilities were  
427 positively correlated with the sulfate concentration, and these correlations were statistically  
428 significant. This implied that sulfate played a key role in the formation of water-soluble Cr, Fe,  
429 Co, Cu, Pb, and Mn, likely through sulfate-driven acid dissolution of their water-insoluble forms.  
430 Conversely, the positive correlations between the sulfate concentration and the Al, Ni, V, and  
431 Cd fractional solubilities were weak and not statistically significant. Interestingly, the V and  
432 Cd fractional solubilities showed weak correlations with the sulfate concentration ( $R = 0.14$   
433 and  $R = 0.04$ , respectively), whereas their water-soluble concentrations showed strong  
434 correlations with the sulfate concentration ( $R = 0.65$  and  $R = 0.74$ , respectively). It is possible  
435 that the strong correlations of sulfate concentration with water-soluble V and Cd concentrations  
436 but not with V and Cd fractional solubilities were due to a large fraction of water-soluble V and  
437 Cd having the same emission sources as the sulfate precursor (i.e., SO<sub>2</sub>).

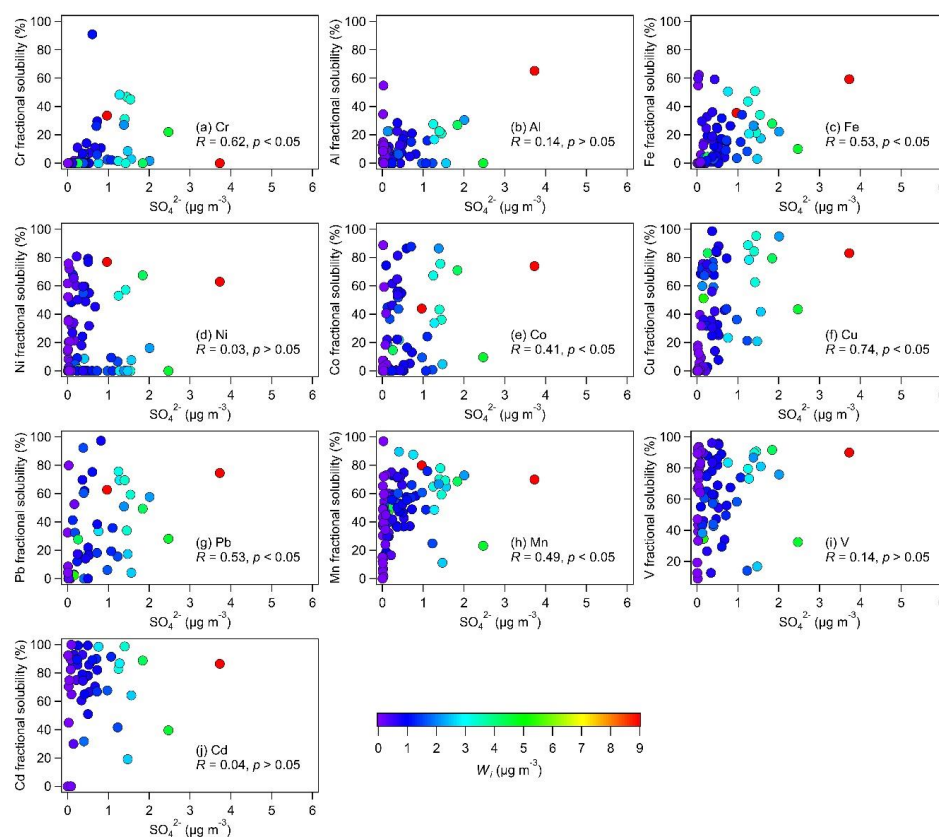
438 **Table 1:** Spearman rank correlations between the metal fractional solubilities and  $W_i$  and  $H_{air}^+$   
439 in fine aerosols<sup>a</sup>

| Metal | Sulfate     | $W_i$       | $H_{air}^+$ |
|-------|-------------|-------------|-------------|
| Cr    | <b>0.62</b> | <b>0.42</b> | <b>0.48</b> |
| Al    | 0.14        | 0.08        | 0.14        |



|    |             |             |             |
|----|-------------|-------------|-------------|
| Fe | <b>0.53</b> | <b>0.31</b> | <b>0.50</b> |
| Ni | 0.03        | 0.01        | 0.18        |
| Co | <b>0.41</b> | <b>0.41</b> | <b>0.23</b> |
| Cu | <b>0.74</b> | <b>0.72</b> | <b>0.24</b> |
| Pb | <b>0.53</b> | <b>0.41</b> | <b>0.34</b> |
| Mn | <b>0.49</b> | <b>0.43</b> | <b>0.23</b> |
| V  | 0.14        | 0.01        | 0.21        |
| Cd | 0.04        | 0.10        | 0.13        |

440 <sup>a</sup> Bold: statistically significant ( $p < 0.05$ )



441

442 **Figure 6:** Relationships between the metal fractional solubilities and sulfate mass  
 443 concentration in fine aerosols. Only data with non-zero total metal concentrations were used in  
 444 the figures. Also shown are the spearman correlation coefficients for each relationship. The  
 445 symbols are colored by the corresponding  $W_i$  concentrations calculated by ISORROPIA-II.  
 446 The  $W_i$  concentrations increased with sulfate concentrations.



447 High levels of aerosol acidity and liquid water are generally needed for the acid  
448 dissolution of metals in an aqueous aerosol particle. In addition to being the main contributor  
449 to aerosol acidity levels (i.e.,  $H_{air}^+$ ), sulfate is a highly hygroscopic species that will influence  
450 the overall aerosol water uptake behavior, which will drive  $W_i$ . Sulfate was the main driver of  
451  $W_i$  in fine aerosols in our study since the mass concentrations of nitrate (another highly  
452 hygroscopic species) were very low (about 18 times lower than sulfate, on average). Both  $W_i$   
453 and  $H_{air}^+$  were controlled primarily by sulfate (sulfate and  $W_i$   $R = 0.90$ ,  $p < 0.05$ ; sulfate and  
454  $H_{air}^+$   $R = 0.63$ ,  $p < 0.05$ ). Thus, we analyzed the relationships between the aerosol metal  
455 fractional solubilities and  $W_i$  and  $H_{air}^+$  (Figures S6 and S7). Table 1 shows that correlations  
456 between the Al, Ni, V, and Cd fractional solubilities and  $W_i$  and  $H_{air}^+$  were weak. Together, the  
457 weak correlations between the fractional solubilities of Al, Ni, V, and Cd and sulfate,  $W_i$ , and  
458  $H_{air}^+$  implied that acid processing may have played a minor role in enhancing the solubilities  
459 of these four metals. Other atmospheric processes beyond acid processing (e.g., cloud  
460 processing, photoreduction) could have played more important roles in enhancing the  
461 solubilities of these four metals (Zhu et al., 1993; Spokes et al., 1994; Kuma et al., 1995). It is  
462 possible that these four metals had slow acid dissolution rates as a result of their mineralogy  
463 and oxidation states. The impacts of mineralogy and oxidation states on the susceptibilities of  
464 water-insoluble Al, Ni, V, and Cd to acid dissolution are currently not known. However,  
465 previous studies showed that different aerosol Fe mineralogy and oxidation states have  
466 different susceptibilities to acid dissolution that will occur at different timescales (Ingall et al.,  
467 2018). Hence, analogous to Fe, it is possible that the mineralogy and oxidation states of Al, Ni,  
468 V, and Cd in the collected aerosols may have resulted in these four metals being less susceptible  
469 to acid processing, which in turn caused them to undergo slow sulfate-driven acid dissolution  
470 from water-insoluble forms to water-soluble forms.

471 Table 1 shows that the Cr, Fe, Co, Cu, Pb, and Mn fractional solubilities were positively  
472 correlated with  $W_i$  and  $H_{air}^+$ , and these correlations were statistically significant. Together, the  
473 strong correlations between the fractional solubilities of Cr, Fe, Co, Cu, Pb, and Mn and sulfate,  
474  $W_i$ , and  $H_{air}^+$  indicated that acid processing likely played a major role in enhancing the  
475 solubilities of these six metals. The fractional solubilities of Co, Cu, Pb, and Mn were more



476 strongly correlated with the  $W_i$  concentration than with the  $H_{air}^+$  concentration. This suggested  
477 that  $W_i$  had a stronger influence on the acid dissolution of Co, Cu, Pb, and Mn. The strong  
478 influence that  $W_i$  has on the metal fractional solubility could be explained by the role of aerosol  
479 water as a reaction medium for the acid dissolution of metals in an aqueous aerosol particle.  
480 Wong et al. (2020) previously showed that at a relatively constant aerosol pH, a decrease in  $W_i$   
481 will lead to a decrease in the reaction medium volume, which in turn will lead to decreases in  
482 the overall formation rates of water-soluble metals. Conversely, the fractional solubilities of Cr  
483 and Fe were more strongly correlated with the  $H_{air}^+$  concentration than with the  $W_i$   
484 concentration. This suggested that the aerosol acidity levels had a stronger influence on the  
485 acid dissolution of Cr and Fe.

486 Interestingly, variability in the aerosol pH did not appear to be a key driver of the  
487 variability in the solubilities of Cr, Fe, Co, Cu, Pb, and Mn. It was difficult to discern aerosol  
488 pH-dependent fractional solubility trends for these six metals, and their fractional solubilities  
489 were not highly correlated with aerosol pH (Figure S8). This could be attributed partly to the  
490 scatter in the datasets caused by differences in the metal solubilities and pH in individual  
491 aerosol particles that would not be captured by the bulk chemical analysis and thermodynamic  
492 modeling performed in this study. The absence of obvious aerosol pH-dependent fractional  
493 solubility trends could also be due to the insensitivity of aerosol pH to the variability of sulfate  
494 ( $R = -0.22$ ,  $p < 0.05$ ). Based on Equation (1), the aerosol pH could be viewed simply as the  
495 ratio of  $H_{air}^+$  and  $W_i$ . Both  $W_i$  and  $H_{air}^+$  were highly variable in this study, and both were  
496 controlled primarily by sulfate. As a result, the ratio of  $H_{air}^+$  and  $W_i$ , or the aerosol pH, would  
497 be fairly insensitive to sulfate even though it was driven primarily by sulfate. Previous studies  
498 have similarly reported weak or the absence of aerosol pH-dependent metal fractional solubility  
499 trends despite evidence of aerosol metal dissolution being enhanced by acid processing (Shi et  
500 al., 2020; Wong et al., 2020).

#### 501 4. Conclusions

502 In this study, we investigated the abundance and fractional solubilities of ten metals (Fe,  
503 Cu, Al, V, Cr, Mn, Co, Ni, Cd, and Pb) in size-fractionated aerosols collected at an urban site



504 in Hong Kong. Weekly aerosol samples were collected for a month during different seasons  
505 from March 2021 to January 2022. The main objective of this study was to identify the key  
506 factors that controlled metal solubilities in fine aerosols, with a focus on aerosol metal  
507 dissolution via the acid processing and metal-organic complexation mechanisms. Hence, other  
508 aerosol chemical species were measured in addition to the total and water-soluble metals.

509 Higher mass concentrations of total metals were usually measured during the winter  
510 and/or spring seasons. This was likely due to the long-range transport of polluted air masses by  
511 northerly prevailing winds from emission sources located in continental areas north of Hong  
512 Kong. The total metals could be arranged in the following order based on their abundances:  
513  $\text{Fe} > \text{Al} > \text{Cu} > \text{Mn} > \text{Pb} > \text{Ni} > \text{Cr} > \text{V} > \text{Co} > \text{Cd}$ . This order of abundance was the same for  
514 both fine and coarse aerosols. The major sources of the total metals were sea salt, dust, ship  
515 emissions, and industrial activities. Higher mass concentrations of water-soluble metals were  
516 also usually measured during the winter and/or spring seasons. With the exception of Cu, the  
517 water-soluble metals had higher mass concentrations in fine aerosols than in coarse aerosols.  
518 The mass concentrations of water-soluble metals generally correlated with the mass  
519 concentrations of total metals, which implied that the water-soluble metals were largely derived  
520 from their total metals through atmospheric processing and/or that water-soluble and water-  
521 insoluble metals have the same emission sources. The study-averaged metal fractional  
522 solubilities spanned a wide range for both fine (8.8 % to 70.3 %) and coarse (1.4 % to 54.3 %)   
523 aerosols. With the exception of Cu and Co, the metals exhibited higher fractional solubilities  
524 in fine aerosols compared to coarse aerosols. The aerosol size-dependent metal fractional  
525 solubility could potentially be attributed to differences in the composition and metal  
526 mineralogy which resulted in different metal dissolution rates and/or mechanisms for aerosols  
527 of different sizes.

528 The fine aerosols collected in this study were mostly acidic, with about 60 % of the  
529 calculated pH values below 3. The acidic nature of the fine aerosols combined with oxalate  
530 (which forms metal-organic complexes easily) not being detected in our aerosol samples  
531 suggested that organic ligand-promoted dissolution likely played a minor role in enhancing  
532 aerosol metal solubilities. This is because organic ligand-promoted metal dissolution is a slow



533 process, and it plays a minor role in metal dissolution under low pH conditions. Our analyses  
534 showed that sulfate, which is the dominant fine aerosol acidic species, exhibited statistically  
535 significant positive correlations with both the water-soluble concentrations of Cr, Fe, Co, Cu,  
536 Pb, and Mn and their fractional solubilities. In addition, sulfate controlled  $W_i$  and  $H_{air}^+$ , both of  
537 which are needed for acid dissolution of metals in an aqueous aerosol particle. The water-  
538 soluble concentrations of Cr, Fe, Co, Cu, Pb, and Mn and their fractional solubilities exhibited  
539 statistically significant positive correlations with both  $W_i$  and  $H_{air}^+$ . Together, the strong  
540 correlations between the fractional solubilities of Cr, Fe, Co, Cu, Pb, and Mn and sulfate,  $W_i$ ,  
541 and  $H_{air}^+$  indicated that acid processing likely played a major role in enhancing the solubilities  
542 of these six metals. The fractional solubilities of Co, Cu, Pb, and Mn were more strongly  
543 correlated with the  $W_i$  concentration than with the  $H_{air}^+$  concentration, which implied that  $W_i$   
544 had a stronger influence on the acid dissolution of these four metals. The fractional solubilities  
545 of Cr and Fe were more strongly correlated with the  $H_{air}^+$  concentration than with the  $W_i$   
546 concentration, which implied that the aerosol acidity levels had a stronger influence on the acid  
547 dissolution of these two metals. Conversely, our analyses suggested that acid processing played  
548 a minor role in enhancing the solubilities of Al, Ni, V, and Cd. It is possible that the mineralogy  
549 and oxidation states of these four metals made them less susceptible to acid processing.

550 In conclusion, this study highlights the key role that sulfate plays in controlling the  
551 solubilities of a host of metals in fine aerosols (in this case, Cr, Fe, Co, Cu, Pb, and Mn). This  
552 is mostly due to sulfate's ability to both strongly acidify the aerosol particle and provide the  
553 liquid reaction medium needed for the acid dissolution of metals. Although this study was  
554 performed at an urban site in Hong Kong, we expect our findings to broadly apply to other  
555 urban areas in Hong Kong and South China, where sulfate is the dominant acidic and  
556 hygroscopic component in fine aerosols. Results from this study can also provide insights into  
557 how the solubilities of different aerosol metals will change with the decrease in sulfate as Hong  
558 Kong and other cities in South China transition away from coal combustion as their main  
559 energy source to improve local and regional air quality and combat climate change.

560 **Data availability:** The data used in this publication is available to the community and can be  
561 accessed at: <https://doi.org/10.5281/zenodo.7013770> (Yang et al., 2022).



562 **Author contributions:** J.Y. and T.N. designed the study. J.Y. collected the field samples. J.Y.,  
563 L.M., and W.C.A. performed chemical analysis of the field samples. J.Y., X.H., Y.M., and T.N.  
564 analyzed the data. J.Y. and T.N. prepared the manuscript with contributions from all co-authors.

565 **Competing interests:** One of the authors is a member of the editorial board of *Atmospheric*  
566 *Chemistry and Physics*. The peer-review process was guided by an independent editor, and the  
567 authors also have no other competing interests to declare.

568 **Acknowledgements:** This work was supported by the Research Grants Council of Hong Kong  
569 (project number 21304919).

## 570 References

571 Adachi, K. and Tainosho, Y.: Characterization of heavy metal particles embedded in tire dust,  
572 *Environment International*, 30, 1009-1017, <https://doi.org/10.1016/j.envint.2004.04.004>, 2004.

573 Al-Abadleh, H. A.: Review of the bulk and surface chemistry of iron in atmospherically  
574 relevant systems containing humic-like substances, *Rsc Advances*, 5, 45785-45811,  
575 <https://doi.org/10.1039/c5ra03132j>, 2015.

576 Al-Abadleh, H. A.: Aging of atmospheric aerosols and the role of iron in catalyzing brown  
577 carbon formation, *Environmental Science: Atmospheres*, 1, 297-345,  
578 <https://doi.org/10.1039/D1EA00038A>, 2021.

579 Baker, A. R. and Jickells, T. D.: Mineral particle size as a control on aerosol iron solubility,  
580 *Geophysical Research Letters*, 33, <https://doi.org/10.1029/2006GL026557>, 2006.

581 Bates, J. T., Fang, T., Verma, V., Zeng, L. H., Weber, R. J., Tolbert, P. E., Abrams, J. Y., Sarnat,  
582 S. E., Klein, M., Mulholland, J. A., and Russell, A. G.: Review of Acellular Assays of Ambient  
583 Particulate Matter Oxidative Potential: Methods and Relationships with Composition, Sources,  
584 and Health Effects, *Environmental Science & Technology*, 53, 4003-4019,  
585 <https://doi.org/10.1021/acs.est.8b03430>, 2019.

586 Birmili, W., Allen, A. G., Bary, F., and Harrison, R. M.: Trace Metal Concentrations and Water  
587 Solubility in Size-Fractionated Atmospheric Particles and Influence of Road Traffic,  
588 *Environmental Science & Technology*, 40, 1144-1153, <https://doi.org/10.1021/es0486925>,  
589 2006.

590 Boyd, P. W., Jickells, T., Law, C. S., Blain, S., Boyle, E. A., Buesseler, K. O., Coale, K. H.,  
591 Cullen, J. J., de Baar, H. J. W., Follows, M., Harvey, M., Lancelot, C., Levasseur, M., Owens,  
592 N. P. J., Pollard, R., Rivkin, R. B., Sarmiento, J., Schoemann, V., Smetacek, V., Takeda, S.,  
593 Tsuda, A., Turner, S., and Watson, A. J.: Mesoscale iron enrichment experiments 1993-2005:  
594 Synthesis and future directions, *Science*, 315, 612-617,





- 595 <https://doi.org/10.1126/science.1131669>, 2007.
- 596 Bresgen, N. and Eckl, P. M.: Oxidative stress and the homeodynamics of iron metabolism,  
597 *Biomolecules*, 5, 808-847, <https://doi.org/10.3390/biom5020808>, 2015.
- 598 Brook, R. D., Rajagopalan, S., Pope, C. A., Brook, J. R., Bhatnagar, A., Diez-Roux, A. V.,  
599 Holguin, F., Hong, Y. L., Luepker, R. V., Mittleman, M. A., Peters, A., Siscovick, D., Smith, S.  
600 C., Whitsel, L., Kaufman, J. D., Amer Heart Assoc Council, E., Council Kidney Cardiovasc,  
601 D., and Council Nutr Phys Activity, M.: Particulate Matter Air Pollution and Cardiovascular  
602 Disease An Update to the Scientific Statement From the American Heart Association,  
603 *Circulation*, 121, 2331-2378, <https://doi.org/10.1161/CIR.0b013e3181d8bec1>, 2010.
- 604 Chen, H. H. and Grassian, V. H.: Iron Dissolution of Dust Source Materials during Simulated  
605 Acidic Processing: The Effect of Sulfuric, Acetic, and Oxalic Acids, *Environmental Science &  
606 Technology*, 47, 10312-10321, <https://doi.org/10.1021/es401285s>, 2013.
- 607 Chow, W. S., Huang, X. H. H., Leung, K. F., Huang, L., Wu, X., and Yu, J. Z.: Molecular and  
608 elemental marker-based source apportionment of fine particulate matter at six sites in Hong  
609 Kong, China, *Science of The Total Environment*, 813, 152652,  
610 <https://doi.org/10.1016/j.scitotenv.2021.152652>, 2022.
- 611 Chu, B., Hao, J., Li, J., Takekawa, H., Wang, K., and Jiang, J.: Effects of two transition metal  
612 sulfate salts on secondary organic aerosol formation in toluene/NO<sub>x</sub>photooxidation, *Frontiers  
613 of Environmental Science & Engineering*, 7, 1-9, <https://doi.org/10.1007/s11783-012-0476-x>,  
614 2013.
- 615 Chu, B., Liggio, J., Liu, Y., He, H., Takekawa, H., Li, S.-M., and Hao, J.: Influence of metal-  
616 mediated aerosol-phase oxidation on secondary organic aerosol formation from the ozonolysis  
617 and OH-oxidation of  $\alpha$ -pinene, *Scientific Reports*, 7, 40311, <https://doi.org/10.1038/srep40311>,  
618 2017.
- 619 Cohen, A. J., Brauer, M., Burnett, R., Anderson, H. R., Frostad, J., Estep, K., Balakrishnan, K.,  
620 Brunekreef, B., Dandona, L., Dandona, R., Feigin, V., Freedman, G., Hubbell, B., Jobling, A.,  
621 Kan, H., Knibbs, L., Liu, Y., Martin, R., Morawska, L., Pope, C. A., Shin, H., Straif, K.,  
622 Shaddick, G., Thomas, M., van Dingenen, R., van Donkelaar, A., Vos, T., Murray, C. J. L., and  
623 Forouzanfar, M. H.: Estimates and 25-year trends of the global burden of disease attributable  
624 to ambient air pollution: an analysis of data from the Global Burden of Diseases Study 2015,  
625 *Lancet*, 389, 1907-1918, [https://doi.org/10.1016/s0140-6736\(17\)30505-6](https://doi.org/10.1016/s0140-6736(17)30505-6), 2017.
- 626 Costa, D. L. and Dreher, K. L.: Bioavailable transition metals in particulate matter mediate  
627 cardiopulmonary injury in healthy and compromised animal models, *Environmental Health  
628 Perspectives*, 105, 1053-1060, <https://doi.org/10.2307/3433509>, 1997.
- 629 de Baar, H. J. W., Boyd, P. W., Coale, K. H., Landry, M. R., Tsuda, A., Assmy, P., Bakker, D.  
630 C. E., Bozec, Y., Barber, R. T., Brzezinski, M. A., Buesseler, K. O., Boye, M., Croot, P. L.,  
631 Gervais, F., Gorbunov, M. Y., Harrison, P. J., Hiscock, W. T., Laan, P., Lancelot, C., Law, C. S.,



- 632 Levasseur, M., Marchetti, A., Millero, F. J., Nishioka, J., Nojiri, Y., van Oijen, T., Riebesell, U.,  
633 Rijkenberg, M. J. A., Saito, H., Takeda, S., Timmermans, K. R., Veldhuis, M. J. W., Waite, A.  
634 M., and Wong, C. S.: Synthesis of iron fertilization experiments: From the iron age in the age  
635 of enlightenment, *Journal of Geophysical Research-Oceans*, 110,  
636 <https://doi.org/10.1029/2004jc002601>, 2005.
- 637 Deguillaume, L., Leriche, M., Desboeufs, K., Mailhot, G., George, C., and Chaumerliac, N.:  
638 Transition Metals in Atmospheric Liquid Phases: Sources, Reactivity, and Sensitive  
639 Parameters, *Chemical Reviews*, 105, 3388-3431, <https://doi.org/10.1021/cr040649c>, 2005.
- 640 Fang, T., Guo, H., Verma, V., Peltier, R. E., and Weber, R. J.: PM<sub>2.5</sub> water-soluble elements in  
641 the southeastern United States: automated analytical method development, spatiotemporal  
642 distributions, source apportionment, and implications for health studies, *Atmos. Chem. Phys.*,  
643 15, 11667-11682, <https://doi.org/10.5194/acp-15-11667-2015>, 2015.
- 644 Fang, T., Guo, H., Zeng, L., Verma, V., Nenes, A., and Weber, R. J.: Highly Acidic Ambient  
645 Particles, Soluble Metals, and Oxidative Potential: A Link between Sulfate and Aerosol  
646 Toxicity, *Environmental Science & Technology*, 51, 2611-2620,  
647 <https://doi.org/10.1021/acs.est.6b06151>, 2017.
- 648 Fountoukis, C. and Nenes, A.: ISORROPIA II: a computationally efficient thermodynamic  
649 equilibrium model for K<sup>+</sup>-Ca<sup>2+</sup>-Mg<sup>2+</sup>-NH<sub>4</sub><sup>+</sup>-Na<sup>+</sup>-SO<sub>4</sub><sup>2-</sup>-NO<sub>3</sub><sup>-</sup>-Cl<sup>-</sup>-H<sub>2</sub>O aerosols,  
650 *Atmos. Chem. Phys.*, 7, 4639-4659, <https://doi.org/10.5194/acp-7-4639-2007>, 2007.
- 651 Fountoukis, C., Nenes, A., Sullivan, A., Weber, R., Van Reken, T., Fischer, M., Matias, E.,  
652 Moya, M., Farmer, D., and Cohen, R. C.: Thermodynamic characterization of Mexico City  
653 aerosol during MILAGRO 2006, *Atmospheric Chemistry and Physics*, 9, 2141-2156,  
654 <https://doi.org/10.5194/acp-9-2141-2009>, 2009.
- 655 Frampton, M. W., Ghio, A. J., Samet, J. M., Carson, J. L., Carter, J. D., and Devlin, R. B.:  
656 Effects of aqueous extracts of PM<sub>10</sub> filters from the Utah Valley on human airway epithelial  
657 cells, *American Journal of Physiology-Lung Cellular and Molecular Physiology*, 277, L960-  
658 L967, <https://doi.org/10.1152/ajplung.1999.277.5.L960>, 1999.
- 659 Gao, D., Mulholland, J. A., Russell, A. G., and Weber, R. J.: Characterization of water-insoluble  
660 oxidative potential of PM<sub>2.5</sub> using the dithiothreitol assay, *Atmospheric Environment*, 224,  
661 <https://doi.org/10.1016/j.atmosenv.2020.117327>, 2020.
- 662 Garg, B. D., Cadle, S. H., Mulawa, P. A., Groblicki, P. J., Laroo, C., and Parr, G. A.: Brake  
663 Wear Particulate Matter Emissions, *Environmental Science & Technology*, 34, 4463-4469,  
664 <https://doi.org/10.1021/es001108h>, 2000.
- 665 Garrett, R. G.: Natural Sources of Metals to the Environment, *Human and Ecological Risk*  
666 *Assessment: An International Journal*, 6, 945-963,  
667 <https://doi.org/10.1080/10807030091124383>, 2000.



- 668 Giorio, C., D'Aronco, S., Di Marco, V., Badocco, D., Battaglia, F., Soldà, L., Pastore, P., and  
669 Tapparo, A.: Emerging investigator series: aqueous-phase processing of atmospheric aerosol  
670 influences dissolution kinetics of metal ions in an urban background site in the Po Valley,  
671 *Environmental Science: Processes & Impacts*, 24, 884-897,  
672 <http://dx.doi.org/10.1039/D2EM00023G>, 2022.
- 673 He, X., Liu, P., Zhao, W., Xu, H., Zhang, R., and Shen, Z.: Size distribution of water-soluble  
674 metals in atmospheric particles in Xi'an, China: Seasonal variations, bioavailability, and health  
675 risk assessment, *Atmospheric Pollution Research*, 12, 101090,  
676 <https://doi.org/10.1016/j.apr.2021.101090>, 2021.
- 677 Heal, M. R., Elton, R. A., Hibbs, L. R., Agius, R. M., and Beverland, I. J.: A time-series study  
678 of the health effects of water-soluble and total-extractable metal content of airborne particulate  
679 matter, *Occupational and Environmental Medicine*, 66, 636-638,  
680 <https://doi.org/10.1136/oem.2008.045310>, 2009.
- 681 Hopke, P. K., Lamb, R. E., and Natusch, D. F. S.: Multielemental characterization of urban  
682 roadway dust, *Environmental Science & Technology*, 14, 164-172,  
683 <https://doi.org/10.1021/es60162a006>, 1980.
- 684 Ingall, E. D., Feng, Y., Longo, A. F., Lai, B., Shelley, R. U., Landing, W. M., Morton, P. L.,  
685 Nenes, A., Mihalopoulos, N., Violaki, K., Gao, Y., Sahai, S., and Castorina, E.: Enhanced Iron  
686 Solubility at Low pH in Global Aerosols, *Atmosphere*, 9, 201,  
687 <https://doi.org/10.3390/atmos9050201>, 2018.
- 688 Jiang, S. Y., Kaul, D. S., Yang, F., Sun, L., and Ning, Z.: Source apportionment and water  
689 solubility of metals in size segregated particles in urban environments, *Science of The Total  
690 Environment*, 533, 347-355, <https://doi.org/10.1016/j.scitotenv.2015.06.146>, 2015.
- 691 Jiang, S. Y. N., Yang, F., Chan, K. L., and Ning, Z.: Water solubility of metals in coarse PM  
692 and PM<sub>2.5</sub> in typical urban environment in Hong Kong, *Atmospheric Pollution Research*, 5,  
693 236-244, <https://doi.org/10.5094/APR.2014.029>, 2014.
- 694 Jordi, A., Basterretxea, G., Tovar-Sanchez, A., Alastuey, A., and Querol, X.: Copper aerosols  
695 inhibit phytoplankton growth in the Mediterranean Sea, *Proceedings of the National Academy  
696 of Sciences of the United States of America*, 109, 21246-21249,  
697 <https://doi.org/10.1073/pnas.1207567110>, 2012.
- 698 Kuma, K., Nakabayashi, S., and Matsunaga, K.: Photoreduction of Fe(III) by  
699 hydroxycarboxylic acids in seawater, *Water Research*, 29, 1559-1569,  
700 [https://doi.org/10.1016/0043-1354\(94\)00289-J](https://doi.org/10.1016/0043-1354(94)00289-J), 1995.
- 701 Lakey, P. S. J., Berkemeier, T., Tong, H. J., Arangio, A. M., Lucas, K., Poschl, U., and Shiraiwa,  
702 M.: Chemical exposure-response relationship between air pollutants and reactive oxygen  
703 species in the human respiratory tract, *Scientific Reports*, 6, <https://doi.org/10.1038/srep32916>,  
704 2016.



- 705 Lippmann, M.: Toxicological and epidemiological studies of cardiovascular effects of ambient  
706 air fine particulate matter (PM<sub>2.5</sub>) and its chemical components: Coherence and public health  
707 implications, *Critical Reviews in Toxicology*, 44, 299-347,  
708 <https://doi.org/10.3109/10408444.2013.861796>, 2014.
- 709 Longo, A. F., Feng, Y., Lai, B., Landing, W. M., Shelley, R. U., Nenes, A., Mihalopoulos, N.,  
710 Violaki, K., and Ingall, E. D.: Influence of Atmospheric Processes on the Solubility and  
711 Composition of Iron in Saharan Dust, *Environmental Science & Technology*, 50, 6912-6920,  
712 <https://doi.org/10.1021/acs.est.6b02605>, 2016.
- 713 Lough, G. C., Schauer, J. J., Park, J.-S., Shafer, M. M., DeMinter, J. T., and Weinstein, J. P.:  
714 Emissions of Metals Associated with Motor Vehicle Roadways, *Environmental Science &  
715 Technology*, 39, 826-836, <https://doi.org/10.1021/es048715f>, 2005.
- 716 Mahowald, N. M., Hamilton, D. S., Mackey, K. R. M., Moore, J. K., Baker, A. R., Scanza, R.  
717 A., and Zhang, Y.: Aerosol trace metal leaching and impacts on marine microorganisms, *Nature  
718 Communications*, 9, 2614, <https://doi.org/10.1038/s41467-018-04970-7>, 2018.
- 719 Mao, J., Fan, S., and Horowitz, L. W.: Soluble Fe in Aerosols Sustained by Gaseous HO<sub>2</sub>  
720 Uptake, *Environmental Science & Technology Letters*, 4, 98-104,  
721 <https://doi.org/10.1021/acs.estlett.7b00017>, 2017.
- 722 Mao, J., Fan, S., Jacob, D. J., and Travis, K. R.: Radical loss in the atmosphere from Cu-Fe  
723 redox coupling in aerosols, *Atmos. Chem. Phys.*, 13, 509-519, [https://doi.org/10.5194/acp-13-  
724 509-2013](https://doi.org/10.5194/acp-13-509-2013), 2013.
- 725 Nriagu, J. O.: A global assessment of natural sources of atmospheric trace metals, *Nature*, 338,  
726 47-49, <https://doi.org/10.1038/338047a0>, 1989.
- 727 Oakes, M., Ingall, E. D., Lai, B., Shafer, M. M., Hays, M. D., Liu, Z. G., Russell, A. G., and  
728 Weber, R. J.: Iron Solubility Related to Particle Sulfur Content in Source Emission and Ambient  
729 Fine Particles, *Environmental Science & Technology*, 46, 6637-6644,  
730 <https://doi.org/10.1021/es300701c>, 2012.
- 731 Paatero, P.: Least squares formulation of robust non-negative factor analysis, *Chemometrics  
732 and Intelligent Laboratory Systems*, 37, 23-35, [https://doi.org/10.1016/S0169-7439\(96\)00044-  
733 5](https://doi.org/10.1016/S0169-7439(96)00044-5), 1997.
- 734 Paatero, P. and Tapper, U.: Positive matrix factorization: A non-negative factor model with  
735 optimal utilization of error estimates of data values, *Environmetrics*, 5, 111-126,  
736 <https://doi.org/10.1002/env.3170050203>, 1994.
- 737 Paris, R. and Desboeufs, K. V.: Effect of atmospheric organic complexation on iron-bearing  
738 dust solubility, *Atmospheric Chemistry and Physics*, 13, 4895-4905,  
739 <https://doi.org/10.5194/acp-13-4895-2013>, 2013.
- 740 Paris, R., Desboeufs, K. V., and Journet, E.: Variability of dust iron solubility in atmospheric



- 741 waters: Investigation of the role of oxalate organic complexation, *Atmospheric Environment*,  
742 45, 6510-6517, <https://doi.org/10.1016/j.atmosenv.2011.08.068>, 2011.
- 743 Paytan, A., Mackey, K. R. M., Chen, Y., Lima, I. D., Doney, S. C., Mahowald, N., Labiosa, R.,  
744 and Postf, A. F.: Toxicity of atmospheric aerosols on marine phytoplankton, *Proceedings of the*  
745 *National Academy of Sciences of the United States of America*, 106, 4601-4605,  
746 <https://doi.org/10.1073/pnas.0811486106>, 2009.
- 747 Phalen, R. F.: The particulate air pollution controversy, *Nonlinearity Biol Toxicol Med*, 2, 259-  
748 292, <https://doi.org/10.1080/15401420490900245>, 2004.
- 749 Pye, H. O. T., Nenes, A., Alexander, B., Ault, A. P., Barth, M. C., Clegg, S. L., Collett Jr, J. L.,  
750 Fahey, K. M., Hennigan, C. J., Herrmann, H., Kanakidou, M., Kelly, J. T., Ku, I. T., McNeill,  
751 V. F., Riemer, N., Schaefer, T., Shi, G., Tilgner, A., Walker, J. T., Wang, T., Weber, R., Xing, J.,  
752 Zaveri, R. A., and Zuend, A.: The acidity of atmospheric particles and clouds, *Atmos. Chem.*  
753 *Phys.*, 20, 4809-4888, <https://doi.org/10.5194/acp-20-4809-2020>, 2020.
- 754 Schroth, A. W., Crusius, J., Sholkovitz, E. R., and Bostick, B. C.: Iron solubility driven by  
755 speciation in dust sources to the ocean, *Nature Geoscience*, 2, 337-340,  
756 <https://doi.org/10.1038/ngeo501>, 2009.
- 757 Sedwick, P. N., Sholkovitz, E. R., and Church, T. M.: Impact of anthropogenic combustion  
758 emissions on the fractional solubility of aerosol iron: Evidence from the Sargasso Sea,  
759 *Geochemistry, Geophysics, Geosystems*, 8, <https://doi.org/10.1029/2007GC001586>, 2007.
- 760 Shelley, R. U., Landing, W. M., Ussher, S. J., Planquette, H., and Sarthou, G.: Regional trends  
761 in the fractional solubility of Fe and other metals from North Atlantic aerosols (GEOTRACES  
762 cruises GA01 and GA03) following a two-stage leach, *Biogeosciences*, 15, 2271-2288,  
763 <https://doi.org/10.5194/bg-15-2271-2018>, 2018.
- 764 Shi, J., Guan, Y., Ito, A., Gao, H., Yao, X., Baker, A. R., and Zhang, D.: High Production of  
765 Soluble Iron Promoted by Aerosol Acidification in Fog, *Geophysical Research Letters*, 47,  
766 e2019GL086124, <https://doi.org/10.1029/2019GL086124>, 2020.
- 767 Sholkovitz, E. R., Sedwick, P. N., Church, T. M., Baker, A. R., and Powell, C. F.: Fractional  
768 solubility of aerosol iron: Synthesis of a global-scale data set, *Geochimica et Cosmochimica*  
769 *Acta*, 89, 173-189, <https://doi.org/10.1016/j.gca.2012.04.022>, 2012.
- 770 Slikboer, S., Grandy, L., Blair, S. L., Nizkorodov, S. A., Smith, R. W., and Al-Abadleh, H. A.:  
771 Formation of Light Absorbing Soluble Secondary Organics and Insoluble Polymeric Particles  
772 from the Dark Reaction of Catechol and Guaiacol with Fe(III), *Environmental Science &*  
773 *Technology*, 49, 7793-7801, <https://doi.org/10.1021/acs.est.5b01032>, 2015.
- 774 Spokes, L. J., Jickells, T. D., and Lim, B.: Solubilisation of aerosol trace metals by cloud  
775 processing: A laboratory study, *Geochimica et Cosmochimica Acta*, 58, 3281-3287,  
776 [https://doi.org/10.1016/0016-7037\(94\)90056-6](https://doi.org/10.1016/0016-7037(94)90056-6), 1994.



- 777 Tao, Y. and Murphy, J. G.: The Mechanisms Responsible for the Interactions among Oxalate,  
778 pH, and Fe Dissolution in PM<sub>2.5</sub>, *ACS Earth and Space Chemistry*, 3, 2259-2265,  
779 <https://doi.org/10.1021/acsearthspacechem.9b00172>, 2019.
- 780 Wang, W., Liu, M., Wang, T., Song, Y., Zhou, L., Cao, J., Hu, J., Tang, G., Chen, Z., Li, Z., Xu,  
781 Z., Peng, C., Lian, C., Chen, Y., Pan, Y., Zhang, Y., Sun, Y., Li, W., Zhu, T., Tian, H., and Ge,  
782 M.: Sulfate formation is dominated by manganese-catalyzed oxidation of SO<sub>2</sub> on aerosol  
783 surfaces during haze events, *Nature Communications*, 12, <https://doi.org/10.1038/s41467-021-22091-6>, 2021.
- 785 Wang, Z. Z., Fu, H. B., Zhang, L. W., Song, W. H., and Chen, J. M.: Ligand-Promoted  
786 Photoreductive Dissolution of Goethite by Atmospheric Low-Molecular Dicarboxylates,  
787 *Journal of Physical Chemistry A*, 121, 1648-1657, <https://doi.org/10.1021/acs.jpca.6b09160>,  
788 2017.
- 789 Wong, J. P. S., Yang, Y., Fang, T., Mulholland, J. A., Russell, A. G., Ebel, S., Nenes, A., and  
790 Weber, R. J.: Fine Particle Iron in Soils and Road Dust Is Modulated by Coal-Fired Power Plant  
791 Sulfur, *Environmental Science & Technology*, 54, 7088-7096,  
792 <https://doi.org/10.1021/acs.est.0c00483>, 2020.
- 793 Ye, D., Klein, M., Mulholland, J. A., Russell, A. G., Weber, R., Edgerton, E. S., Chang, H. H.,  
794 Sarnat, J. A., Tolbert, P. E., and Ebel, S.: Estimating Acute Cardiovascular Effects of  
795 Ambient PM<sub>2.5</sub> Metals, *Environmental Health Perspectives*, 126, 027007,  
796 <https://doi.org/10.1289/ehp2182>, 2018.
- 797 Zhang, H., Li, R., Dong, S., Wang, F., Zhu, Y., Meng, H., Huang, C., Ren, Y., Wang, X., Hu,  
798 X., Li, T., Peng, C., Zhang, G., Xue, L., Wang, X., and Tang, M.: Abundance and Fractional  
799 Solubility of Aerosol Iron During Winter at a Coastal City in Northern China: Similarities and  
800 Contrasts Between Fine and Coarse Particles, *Journal of Geophysical Research: Atmospheres*,  
801 127, e2021JD036070, <https://doi.org/10.1029/2021JD036070>, 2022.
- 802 Zhao, Z., Luo, X. S., Jing, Y. S., Li, H. B., Pang, Y. T., Wu, L. C., Chen, Q., and Jin, L.: In vitro  
803 assessments of bioaccessibility and bioavailability of PM<sub>2.5</sub> trace metals in respiratory and  
804 digestive systems and their oxidative potential, *Journal of Hazardous Materials*, 409,  
805 <https://doi.org/10.1016/j.jhazmat.2020.124638>, 2021.
- 806 Zhong, L., Louie, P. K. K., Zheng, J., Yuan, Z., Yue, D., Ho, J. W. K., and Lau, A. K. H.:  
807 Science-policy interplay: Air quality management in the Pearl River Delta region and Hong  
808 Kong, *Atmospheric Environment*, 76, 3-10, <https://doi.org/10.1016/j.atmosenv.2013.03.012>,  
809 2013.
- 810 Zhou, Y., Zhang, Y., Griffith, S. M., Wu, G., Li, L., Zhao, Y., Li, M., Zhou, Z., and Yu, J. Z.:  
811 Field Evidence of Fe-Mediated Photochemical Degradation of Oxalate and Subsequent Sulfate  
812 Formation Observed by Single Particle Mass Spectrometry, *Environmental Science &*  
813 *Technology*, 54, 6562-6574, <https://doi.org/10.1021/acs.est.0c00443>, 2020.



- 814 Zhu, X., Prospero, J. M., Savoie, D. L., Millero, F. J., Zika, R. G., and Saltzman, E. S.:  
815 Photoreduction of iron(III) in marine mineral aerosol solutions, *Journal of Geophysical*  
816 *Research: Atmospheres*, 98, 9039-9046, <https://doi.org/10.1029/93JD00202>, 1993.
- 817 Zhu, Y., Li, W., Lin, Q., Yuan, Q., Liu, L., Zhang, J., Zhang, Y., Shao, L., Niu, H., Yang, S., and  
818 Shi, Z.: Iron solubility in fine particles associated with secondary acidic aerosols in east China,  
819 *Environmental Pollution*, 264, 114769, <https://doi.org/10.1016/j.envpol.2020.114769>, 2020.
- 820